Synthesis, Structure, and Reactivity of dealloyed bimetallic PtM$_3$ fuel cell cathode electrocatalysts

Mehtap Oezaslan [b], Stefan Rudi[b], Zengcai Liu[a], Peter Strasser[a,b]

[a]*Center for Nanophase Materials Science, Oak Ridge National Laboratory, Oak Ridge, TN, USA*

[b]*The Electrochemical Energy, Catalysis, and Materials Science Laboratory, Department of Chemistry, Chemical Engineering Division, Technical University Berlin, 10623 Berlin, Germany*

Introduction

Dealloying, the preferential dissolution of the less noble (more reactive) component from a bimetallic alloy, has traditionally been studied in the field of corrosion science[1]. Despite Raney's early reports on advantages of dealloyed catalysts, it was only recently that atomic-scale surface science studies of the dealloyed catalyst structure and the origin of the catalytic properties of dealloyed surfaces have intensified.

We have shown that dealloying of Cu-rich Pt-Cu nanoparticles results in highly active core-shell catalysts for the electroreduction of molecular oxygen for use in fuel cell cathodes (Figure 1) [2-6]. The cores are predominately PtM-alloys, while the shells (surface) are near-pure Pt. A combination of energy-dispersive X-ray analysis (EDX), X-ray diffraction (XRD), and X-ray photoelectron spectroscopy (XPS) was used to probe the chemical and morphological properties of these catalysts. A lattice mismatch between the PtM-alloy core and the Pt shell results in a strained Pt surface. This surface strain leads to a slight weakening of the Pt-O bond strength thereby increasing the turnover frequency for the oxygen reduction reaction (ORR). In half-cell as well as single cell tests the cathode catalysts have shown mass activities in excess of 4x of state-of-the-art Pt/C electrocatalysts; as such, they represent the most active nanoparticle ORR catalysts to date and offer great promise in the lowering of the Pt loadings of hydrogen fuel cells.

In the presentation we will share recent progress in our efforts to characterize dealloyed bimetallics at the atomic scale and understand the origin of the enhanced electrocatalysis. In particular, we will focus on a comparison between the structural aspects of dealloyed PtCu$_3$ and PtCo$_3$ nanoparticle systems, on the dealloying of PtCu3 films as well as on the reactivity and structural aspects of a number of other dealloyed PtM$_3$ systems (M=Cu, Co, Fe, Ni, V).

Experimental

Nanoparticle PtCu3 and PtCo3 and other PtM3 precursors were prepared via an impregnation/freeze drying/annealing procedure. PtCu3 films were sputtered on glassy carbon substrates. Films and particles were subsequently dealloyed electrochemically using a RDE set-up. Electrocatalytic activity was measured in liquid 0.1 M HClO4. X-ray diffraction, Transmission Electron Microscopy (TEM), STEM/EDX, as well as EELS were performed to evaluate the core shell structure of the nanoparticle catalysts

Results and Discussion

HAADF images (Figure 2) and EDX/EELS mappings demonstrated a core shell structure of the dealloyed nanoparticles supporting the initial structural hypothesis. Anomalous XRD yielded compressive strain estimates of <= 5 % for the Cu richest precursors. Strain values correlated well with ORR activity. Anomalous XRD of dealloyed PtCu3 films showed an alloy reflection of the film bulk as well as a broad smaller reflection corresponding to Pt enriched surface layers. Due to the thickness of the dealloyed surface layers, reduced compressive strain values of about 1% were experimentally determined. This data couple agrees excellently with DFT prediction of ORR activity as function of compressive strain in well defined Pt surfaces.

Fig. 3 presents the normalizedECSA-based and Pt-mass based Tafel plots,obtained from the kinetic current jkin for pretreated PtCo3 and PtCu3 catalysts and compared to those for 28.2wt.% Pt/HSAC. The Tafel plots reveal the considerable improvement of intrinsic activities for all Pt–Co and Pt–Cu alloy catalysts. It is seen, that the Tafel slope for ORR changes continuously in the examined potential range. The experimental data exhibits two Tafel slopes at low current density (lcd) and high current density (hcd) region and compared to those from the literature.

Figure 3, (a) Pt ECSA-based Tafel plots of pretreated PtCo3/HSAC, annealed at 650∘C, 800 ∘C and 900∘C for 7 h and pretreated PtCu3/HSAC (800∘C/7h) compared with pure 28.2 wt.% Pt/HSAC. (b) Pt mass-based Tafel plots of pretreated PtCo3/HSAC, annealed at 650 ∘C, 800 ∘C and900 ∘C for 7h and pretreated PtCu3/HSAC (800 ∘C /7 h) compared with pure 28.2wt.% Pt/HSAC.
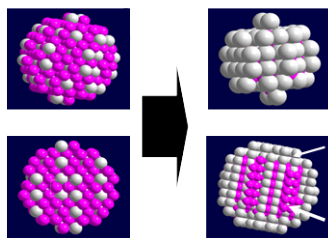

Figure 1, Dealloyed Pt-Cu nanoparticle electrocatalyst show high Pt mass based activity for the electroreduction of oxygen in Fuel cell cathodes. Dealloying is partial removal of less active component from alloy resulting in a core shell structure.
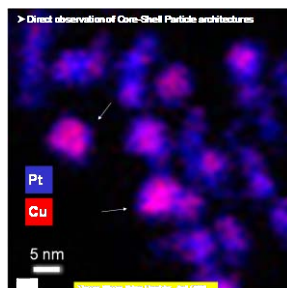

Figure 2, STEM EDX mapping of a dealloyed core shell Pt-Cu electrocatalysts. A blue halo around each particle indicated a Pt enriched surface region. Compressive strain, caused by the alloy core results in reduced chemisorption of oxygenated intermediates and incrases the catalytic rate and activity of the particles
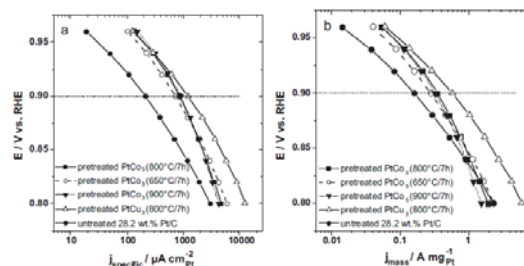
Conclusions

This work is a comparative study of the electrochemical ORR activity of dealloyed PtCu3, PtCo$_3$ and selected PtM3 alloy nanoparticle electrocatalysts, all compared to pure nanoparticle Pt catalysts. We conclude that dealloying of M rich PtM3 precursors results in active ORR catalysts as long as M is a metal with a dimatere smaller than Pt. Correlations between metal M diameter and the specific Pt area normalized activity suggest a geometric effect in the improved ORR catalysis, in line with earlier hypothesis about the presence of surface compressive strain in improved ORR Pt bimetallic catalysts.

Acknowledgement

References

(1)   Erlebacher, J.; Aziz, M. J.; Karma, A.; Dimitrov, N.; Sieradzki, K. *Nature* **2001**, *410*, 450-453.
(2)   Strasser, P.; Koh, S.; Anniyev, T.; Greeley, J.; More, K.; Yu, C.; Liu, Z.; Kaya, S.; Nordlund, D.; Ogasawara, H.; Toney, M. F.; Nilsson, A. *Nature Chem.* **2010**, *2*, 454 - 460.
(3)   Strasser, P. *Rev. Chem. Eng.* **2009**, *25*, 255-295.
(4)   Strasser, P.; Koh, S.; Greeley, J. *Phys. Chem Chem. Phys.* **2008**, *10*, 3670-3683.
(5)   Koh, S.; Strasser, P. *J. Am. Chem. Soc.* **2007**, *129*, 12624-12625.
(6)   Yu, C.; Koh, S.; Leisch, J.; Toney, M. T.; Strasser, P. *Faraday Discuss.* **2008**, *140*, 283-296.